Neuro-Oncology Advances

6(1), vdae056, 2024 | https://doi.org/10.1093/noajnl/vdae056 | Advance Access date 5 April 2024

[11C]-methionine positron emission tomography in the evaluation of pediatric low-grade gliomas

Emily Y. Kim, Amy L. Vavere, Scott E. Snyder, Jason Chiang, Yimei Li, Tushar Patni, Ibrahim Qaddoumi, Thomas E. Merchant, Giles W. Robinson, Joseph L. Holtrop, Barry L. Shulkin†, and Asim K. Bag†,

All author affiliations are listed at the end of the article

Present address: Molecular Imaging Ligand Development Program, Department of Radiology and Imaging Sciences, Indiana University School of Medicine, Indianapolis, Indiana, USA (S.E.S.)

Corresponding Author: Asim K. Bag, MBBS, MD, EDiNR, Department of Diagnostic Imaging, 262 Danny Thomas Place, Mail Stop 220, Memphis, TN 38105, USA (asim.bag@stjude.org).

†Senior Authors: Asim K. Bag and Barry Shulkin.

Abstract

Background. [11C]-Methionine positron emission tomography (PET; [11C]-MET-PET) is principally used for the evaluation of brain tumors in adults. Although amino acid PET tracers are more commonly used in the evaluation of pediatric brain tumors, data on [11C]-MET-PET imaging of pediatric low-grade gliomas (pLGG) is scarce. This study aimed to investigate the roles of [11C]-MET-PET in the evaluation of pLGGs.

Methods. Eighteen patients with newly diagnosed pLGG and 26 previously treated pLGG patients underwent [11C]-MET-PET met the inclusion and exclusion criteria. Tumor-to-brain uptake ratio (TBR) and metabolic tumor volumes were assessed for diagnostic performances (newly diagnosed, 15; previously treated 26), change with therapy (newly diagnosed, 9; previously treated 7), and variability among different histology ($n = 12$) and molecular markers ($n = 7$) of pLGGs.

Results. The sensitivity of [11C]-MET-PET for diagnosing pLGG, newly diagnosed, and previously treated combined was 93% for both TBR_{max} and TBR_{peak}, 76% for TBR_{mean}, and 95% for qualitative evaluation. TBR_{max} showed a statistically significant reduction after treatment, while other PET parameters showed a tendency to decrease. Median TBR_{max}, TBR_{peak}, and TBR_{mean} values were slightly higher in the BRAFV600E mutated tumors compared to the BRAF fused tumors. Median TBR_{max}, and TBR_{peak} in diffuse astrocytomas were higher compared to pilocytic astrocytomas, but median TBR_{mean}, was slightly higher in pilocytic astrocytomas. However, formal statistical analysis was not done due to the small sample size.

Conclusions. Our study shows that [11C]-MET-PET reliably characterizes new and previously treated pLGGs. Our study also shows that quantitative parameters tend to decrease with treatment, and differences may exist between various pLGG types.

Key Points

- MET-PET can be considered as a supporting imaging modality when magnetic resonance imaging is inconclusive.
- MET-PET has very high sensitivity for diagnosis of new and recurrent pLGG.

Tumors of the central nervous system (CNS) are the most common solid tumors in children.[1] Among these tumors, pediatric low-grade gliomas (pLGGs) represent approximately one-third of all pediatric CNS tumors.[2] These gliomas are a heterogeneous group. The current World Health Organization CNS tumor classification scheme classifies pLGGs based on tumor molecular alterations and histopathology.[1,3–5] Treatment decisions now incorporate molecular markers as they better

Importance of the Study

This study is significant because it demonstrates that [11C]-MET-positron emission tomography (PET) is a reliable imaging modality for evaluating pediatric low-grade gliomas (pLGGs), a field that has very limited amino acid PET imaging data. With a high sensitivity demonstrated in both new and previously treated pLGG cases, [11C]-MET-PET emerges as a reliable tool for evaluating these tumors. It provides insight into the metabolic activity of pLGGs, offering a potential metric for assessing treatment efficacy, given the observed reduction in uptake post-therapy. Additionally, the study suggests that [11C]-MET-PET may differentiate between pLGG histologic phenotypes and genotypes, particularly noting variations in tumors with BRAF mutations. These findings could lead to more personalized treatment plans by allowing more precise diagnosis and treatment monitoring to offer better outcomes, marking a significant step in pediatric neuro-oncology.

correlate with the overall prognosis. We now know that pLGGs are commonly derived either from genetic rearrangement (duplication or fusion) of *BRAF* gene or single-nucleotide variant (SNV) of *BRAF* gene (BRAF pV600E), and tumors driven by *BRAF* fusion differ epidemiologically and prognostically from tumors driven by *BRAF* SNV.[6,7]

Gross total resection offers the best survival potential for those with pLGGs, with an 8-year overall survival (OS) rate of 96%,[8] often without any adjuvant therapy.[5] If gross total resection is not feasible, residual tumors can progress, more commonly in SNV-related tumors, and may require additional chemotherapy, radiation therapy, or both.[9] The progression-free survival (PFS) rate is dramatically lower in SNV-related with a 5-year PFS rate of 30% to 40%, compared to pLGGs with genetic rearrangement, which have a 5-year PFS rate of nearly 100%.[6] Children with a less-favorable outcome require multiple therapies over time for tumor control.[10] Vigilant monitoring of response and early detection of tumor progression and recurrence are essential in these children.

Although magnetic resonance imaging (MRI) is the principal imaging modality for management of pLGGs, accurate characterization of pLGG can be challenging with MRI due to slow growth and lack of any specific imaging biomarker on the advanced MRI techniques. Pseudoprogression can also complicate MRI evaluation, although has a much lower incidence in pLGGs as compared to high-grade gliomas.[11] Clinicians often feel the need for better tumor characterization.[12–14] Positron emission tomography (PET) with radio-labeled amino acids is an excellent imaging technique for evaluating low-grade gliomas and has been used primarily in adults.[13,15] [18F]-Fluorodeoxyglucose (FDG) was among the initial radiotracers employed for brain tumor imaging, aiming to detect heightened glucose metabolic activity in gliomas. However, its effectiveness was limited by the naturally high physiological glucose metabolism in the brain. Consequently, other radiotracers [[11C]-methionine ([11C]-MET), [18F]-fluoroethyl-L-tyrosine (FET), [18F]-fluorodopa (FDOPA)] were found to be advantageous over [18F]-FDG with higher sensitivity and specificity due to higher tumor-to-normal brain (NB) contrast than FDG.[16,17] Amino acid PET imaging with [11C]-MET, [18F]-FET, and [18F]-FDOPA has been used in adults to delineate glioma extent,[18] direct biopsy,[19] grade glioma,[18] differentiate glioma recurrence from treatment-induced changes,[18,20] assess treatment response,[18,21] and assess prognosis.[18,22] PET with [18F]-DOPA can also better discriminate low-grade from high-grade pediatric gliomas and is an independent predictor of outcome.[23] Similarly, PET with [18F]-FET can also discriminate tumors from nontumorous lesions in pediatric brain tumors[24] and guide surgery[25] and clinical management.[26,27] Due to added value, a new practice guideline has been developed and endorsed European Association of Nuclear Medicine (EANM), Society of Nuclear Medicine and Molecular Imaging, European Society for Pediatric Oncology (SIOPE) Brain Tumor Group and the Response Assessment in Pediatric Neuro-Oncology (RAPNO) working group for amino acid PET imaging in evaluation of pediatric brain tumors.[28] Of these 3 amino acid and amino acid-like PET tracers, [11C]-MET has been the most extensively investigated. The uptake of [11C]-MET provides a clearer delineation of the gross tumor volume (TV) for low-grade tumors compared to MRI or [18F]-FDG PET.[29,30] and better correlates with histopathology of LGG,[31] tumor cell proliferation (Ki-67 expression and number of viable tumor cells), micro-vessel density,[32] and outcome predictions.[33] [11C]-MET-PET can also differentiate gliomas from non-tumor brain lesions with a high positive predictive value of 96%[34,35] and is considered a reliable biomarker of active brain tumors.[32]

Amino acid PET imaging data in pLGG is scarce compared to adult gliomas. Bag et al.[13] have evaluated the effectiveness of [11C]-MET-PET in pediatric high-grade glioma recurrences and have shown its sensitivity and accuracy to exceed those of MRI. Tinkle et al.[36] demonstrated efficacy of [11C]-MET-PET in diffuse intrinsic pontine glioma. Detecting aggressiveness of pediatric high-grade gliomas has also been evaluated with [11C]-MET-PET.[37] However, no studies have specifically investigated role of [11C]-MET-PET imaging in pLGG.

This report delves into the examination of [11C]-MET-PET's capabilities in diagnosing and characterizing new and recurrent pLGGs. We hypothesize that [11C]-MET-PET will add value to MRI findings in evaluating lesions suspicious for pLGG. Additionally, we investigate the potential changes in [11C]-MET uptake during therapy and whether variations in [11C]-MET uptake exist among different pLGG histologic phenotypes and genotypes.

Materials and Methods

Study Subjects

The study population was identified from all the patients with pLGGs who were enrolled in the "Methionine

PET/CT Studies in Patients with Cancer" clinical trial (NCT00840047) at St. Jude Children's Research Hospital between 2009 and 2019. St. Jude Children's Research Hospital Institutional Review Board approved this study, and each patient or their parent or legal guardian signed informed consent and assent (7–13 years) forms. Forty-nine consecutive pLGG patients (20 males, 29 females; aged 1–26 years) who were enrolled in this study and had [11C]-MET-PET performed within 8 weeks of an MRI scan were included for analysis and divided into 2 groups: Newly diagnosed pLGG and previously treated pLGG. One patient was classified into both newly diagnosed and previously treated cohorts at 2 distinct times and was considered as 2 separate enrollments.

The newly diagnosed group consisted of 21 patients (12 males, 9 females; aged 3-25 years). We excluded 3 patients with spinal pLGG for homogeneity of the data. Within 6 months of [11C]-MET-PET, 15 of the 18 patients had either tumor resection or biopsy that confirmed the diagnosis of pLGG. Quantitative and qualitative assessments of [11C]-MET-PET data of these 15 subjects were analyzed to assess [11C]-MET-PET's diagnostic performance in correctly diagnosing pLGG. [11C]-MET-PET data from 12 of these 15 subjects, who did not receive any chemotherapy or radiation therapy between the [11C]-MET-PET scan and the biopsy or resection, were used to determine differences in [11C]-MET uptake patterns among various genotypes and histologic phenotypes of pLGG. Nine patients from the newly diagnosed group had both a pre- and post-therapy [11C]-MET-PET scans after completing radiation therapy or a course of chemotherapy or a combination of radiation and chemotherapy; pre-and post-therapy quantitative [11C]-MET-PET parametric data of these patients were analyzed to determine therapy-associated changes in [11C]-MET uptake patterns.

The 28 patients in the previously treated group (8 males, 20 females; aged 1–26 years) had either resection or one or more courses of chemotherapy with or without radiation therapy, or both (Supplementary Table 1), and [11C]-MET-PET was performed to evaluate pLGG recurrence. Two patients with spinal pLGG were excluded. Within 6 months of the [11C]-MET-PET, all 26 patients had either biopsy or resection ($n = 11$) or series of follow-up MRI ($n = 15$) or both to confirm the presence of pLGG. Quantitative [11C]-MET-PET parametric data and qualitative assessment of these 26 patients were analyzed to assess [11C]-MET-PET's utility in correctly diagnosing pLGG. Quantitative [11C]-MET-PET parametric data of 7 patients who had either biopsy or resection following [11C]-MET-PET scan and received no therapy between the scan and biopsy were analyzed to determine whether differences between different histologic phenotypes and genotypes of pLGG exist. Seven patients from the recurrent group had a pre- and a post-therapy [11C]-MET-PET after completion of either radiation therapy or a course of chemotherapy. Pre- and post-therapy quantitative [11C]-MET-PET parametric data of these 7 patients were analyzed to determine therapy-associated change in MET uptake patterns.

Analyses of diagnostic performance of quantitative [11C]-MET-PET parameters and subjective evaluation of [11C]-MET-PET and variability between different genotypes and histologic phenotypes of both cohorts were combined for comprehensive analyses. A complete summary of patient distribution and [11C]-MET-PET analyses is shown in Figure 1.

Image Acquisition

Magnetic resonance imaging.—Of the sequences obtained during standard-of-care MRI, we analyzed T2 fluid-attenuated inversion recovery (FLAIR) sequences obtained after administration of a 0.1 mmol/kg gadobutrol (Gadovist; Bayer Healthcare) with the following image parameters: 4 mm slice thickness, no gap, 10 000 ms repetition time, 106 ms echo time, 2600 ms inversion time, and 130° flip angle. Images were obtained by using either 1.5-T (Avanto, Siemens Medical Solutions) or 3-T (Skyra or Prisma, Siemens Medical Solutions) MR systems.

Positron emission tomography.—*L*-[methyl-11C]methionine was synthesized in the Molecular Imaging Core at St. Jude Children's Research Hospital as described previously.[38] All patients underwent at least 4 hours of fasting before scanning. Each patient was injected with 740 MBq (20 mCi) of [11C]-MET radiotracer per 1.7 m^2 of body surface area. The maximum prescribed dose of [11C]-MET was 740 MBq. After 5–15 minutes, transmission CT images and PET images were obtained by using a Discovery 690 PET/CT scanner or a Discovery LS PET/CT scanner (GE Healthcare). The following parameters were selected for the study: Field of view, 30 cm; matrix, 192 × 192; reconstruction method, VUE point HD; quantification method, SharpIR; filter cutoff, 5.0 mm; subsets, 34; iterations, 4; and z-axis filter, standard. The CT acquisition parameters were set as follows: 0.5 cm slice thickness, 0.8 s tube rotation, 1.5 cm/rotation table speed, 1.5:1 pitch, 120 kV, and 90 mA with dose modulation. The 3-dimensional mode was used for 15 minutes when obtaining PET images.

Qualitative imaging analysis.—MET-PET images were independently reviewed by an experienced pediatric molecular imaging physician (BLS) with more than 30 years of experience (Supplementary Tables 2 and 3). The [11C]-MET-PET images were rated qualitatively on a 4-point scale relative to frontal white matter, as previously described.[13] Briefly, images were qualitatively assessed using a 4-point scale based on the uptake level relative to tumor-free areas of frontal white matter. The scale was defined as follows: 0 for no detectable uptake, 1 for mild uptake but less than in the contralateral frontal lobe white matter, 2 for mild uptake similar to that in the contralateral frontal lobe white matter, and 3 for uptake greater than in the contralateral frontal lobe white matter. The visual assessment outcomes were then simplified into 2 categories: The first category included grades 0, 1, and 2, indicating negative and the second category included grade 3, indicating positive.

Quantitative imaging analysis.—Quantitative imaging analysis followed the most recent joint EANM/ SIOPE/ RAPNO EANM/SNMMI practice guidelines and procedure standards.[28] Briefly, the PET images were co-registered

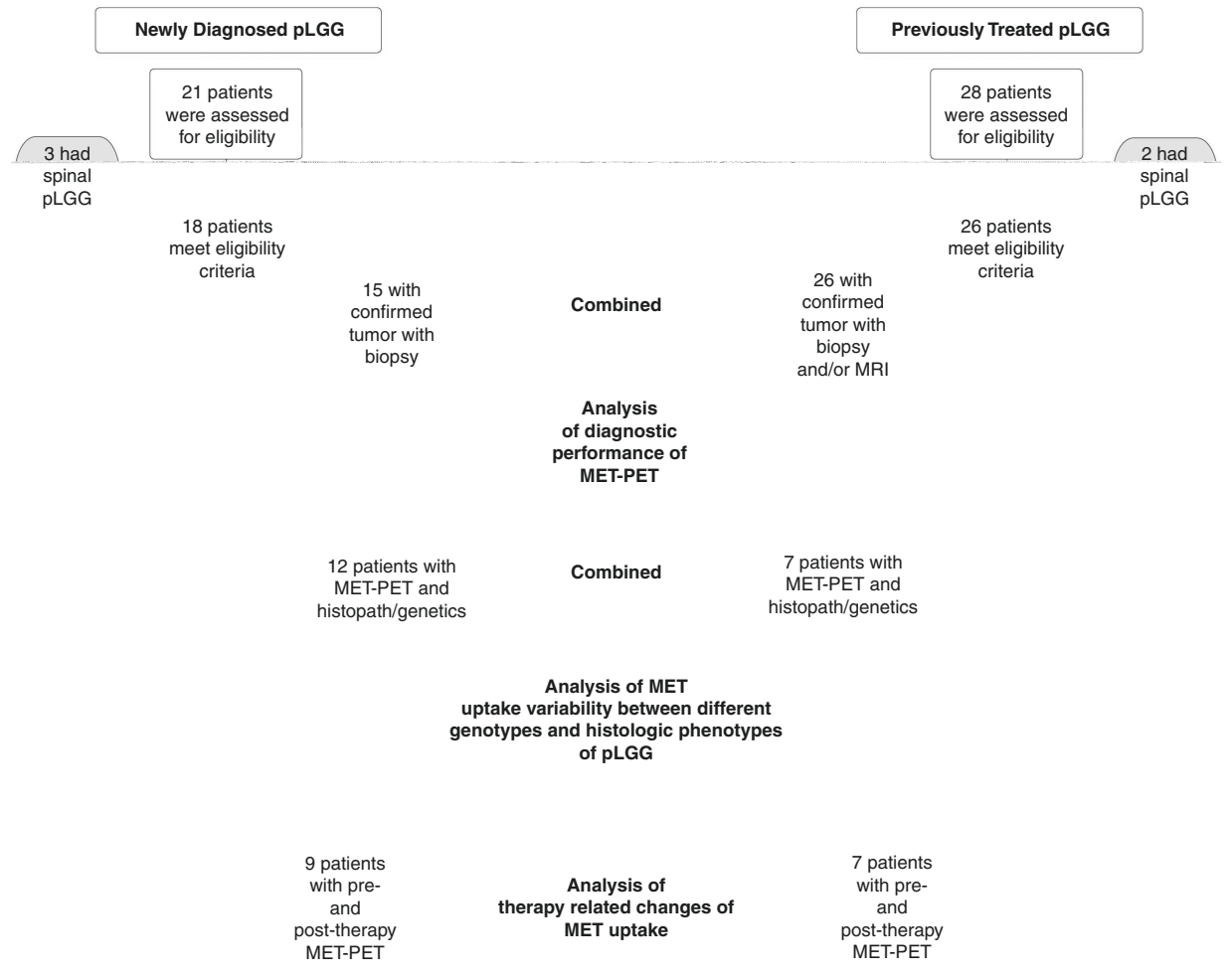

Figure 1. Patient Enrollment and [11C]-MET-positron emission tomography analyses. pLGG, pediatric low-grade glioma.

with the T2 FLAIR images; the tumor was segmented on T2 FLAIR images; and standardized uptake values of the tumor and NB, tumor-to-brain ratio, and metabolic TV (MTV) were calculated. Quantitative analysis was performed using Hermes Medical Solution, Affinity Viewer 3.0.1 (Hermes Medical Solutions, Stockholm, Sweden). Image registration and tumor segmentation were individually verified in each subject by an experienced pediatric neuroradiologist with more than 11 years of experience. SUV of NB[39] was calculated using a 1.0 cm^3 sphere volume of interest (VOI) placed at the juxta-cortical region of the contralateral frontal lobe at the level of centrum semiovale that included both gray matter and white matter, as previously described.[13,20] The MTV was automatically contoured by the Hermes Affinity software, with the constraints of the segmented TV on the T2 FLAIR image using the threshold SUV of > 1.3 times the SUV_{mean} of the NB VOI, as previously described.[13,20,40] SUV_{max}, SUV_{mean}, and SUV_{peak} were calculated for NB, TV, and MTV VOI. Tumor-to-background ratio (TBR) was calculated as a ratio of tumor SUV_{max}, SUV_{mean}, and SUV_{peak} to SUV_{mean} of NB VOI. We compared TV, MTV, TBR_{max}, TBR_{peak}, and TBR_{mean} of pLGGs with *BRAF V600E* with those of pLGGs with *BRAF* duplication or fusion. We also compared these quantitative PET parameters of pilocytic astrocytoma with those of diffuse astrocytoma.

Diagnostic performance analysis.—Sensitivity was calculated to examine the diagnostic performance of PET parameters, TBR_{peak}, and TBR_{mean}, as well as the subjective evaluation of PET by experienced pediatric neuroradiologists. [11C]-MET-PET images were considered positive if TBR > 1.3, and negative if TBR ≤ 1.3. The presence of tumor was confirmed on biopsy, resection, or MRI within 3 months of [11C]-MET-PET. Sensitivity was determined by dividing the number of patients with TBR > 1.3 by the total number of patients with confirmed pLGG.

Histology and molecular analysis.—Hematoxylin and eosin stained 5 µm sections of formalin-fixed, paraffin-embedded (FFPE) tissue specimens were centrally reviewed by board-certified neuropathologists specializing in pediatric CNS tumors to confirm the histologic diagnosis. *BRAF V600E* (Ventana, #790-4855, pre-diluted) antibody was used for immunohistochemistry in a Clinical Laboratory Improvement Amendments-certified laboratory. Reverse

transcription-polymerase chain reaction (RT-PCR) with primer sets to detect 9 reported variants of *KIAA1549:BRAF* fusion or fluorescence in situ hybridization to detect chromosome 7q34 duplication, a marker for *KIAA1549::BRAF* fusion, were performed in a Clinical Laboratory Improvement Amendments-certified laboratory.

Statistical Analysis

A sign test was used to investigate the changes of [11C]-MET uptake following therapy. The analyses were not corrected for multiple comparisons due to their exploratory nature and limited number of observations. All statistical analyses were done using R Statistical Software (R Foundation for Statistical Computing).

Results

Diagnostic Performance of [11C]-MET-PET

The mean TBR_{max}, TBR_{mean}, and TBR_{peak} values of all the newly diagnosed tumors (n = 15) were 3.00 (SD ± 1.83), 1.58 (± 0.54), and 2.58 (± 1.50), respectively (Figure 2). The respective median TBR_{max}, TBR_{mean}, and TBR_{peak} of the newly diagnosed tumors were 2.8. 1.4, and 1.9. Similarly, the mean TBR_{max}, TBR_{mean}, and TBR_{peak} values for all the previously treated tumors ($n = 26$) were 2.53 (± 0.81), 1.50 (± 0.41), and 2.09 (± 0.61; Figure 2). The respective median TBR_{max}, TBR_{mean}, and TBR_{peak} of the previously treated tumors were 2.4. 1.5, and 2.0. The diagnostic performance of qualitative (Figures 3 and 4) and quantitative assessment of [11C]-MET PET is listed in Table 1, and Supplementary Tables 2 and 3.

Changes in [11C]-MET Uptake Following Therapy

In a subgroup analysis, there was a noticeable trend of decreasing quantitative PET parameters and MRI volume (Table 2, and Supplementary Table 4) both in the newly diagnosed ($n = 9$) and in the previously treated group ($n = 7$). However, it did not reach statistical significance, except for the change of TBR_{max} from pretherapy to post-therapy in the combined group. There was also a trend of decreasing FLAIR TV from pretherapy to post-therapy. (Table 2, and Supplementary Table 4)

Comparison of PET Parameters of Histologic and Genetic Variants of pLGG

In the *BRAF V600E* ($n = 2$) group, the median values of $TBR_{max,}$ $TBR_{mean,}$ and TBR_{peak} were higher compared to

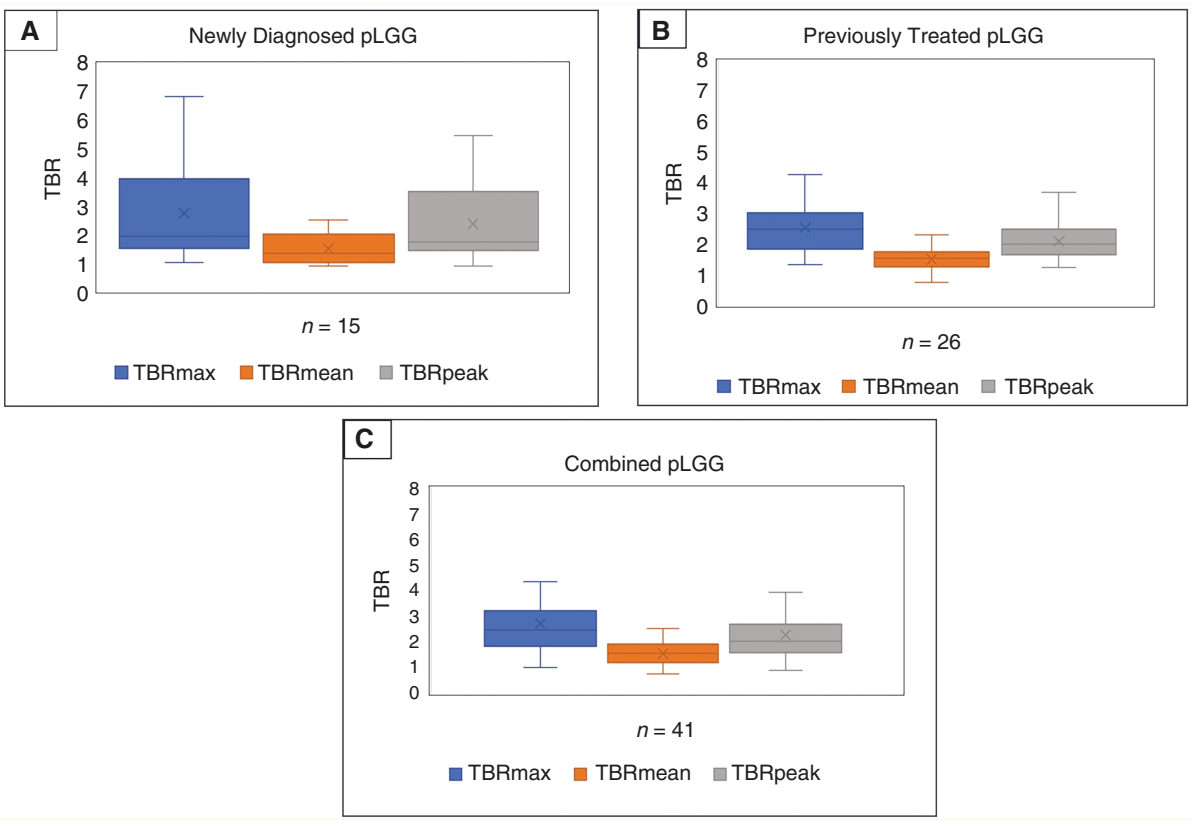

Figure 2. Box and whisker plots of TBR_{max} (blue), TBR_{mean} (orange), and TBR_{peak} (gray) in newly diagnosed (A), previously treated (B) and combined (C) pLGG cohorts. Y-axis: Tumor-to-Brain ratio ([11C]-MET uptake).

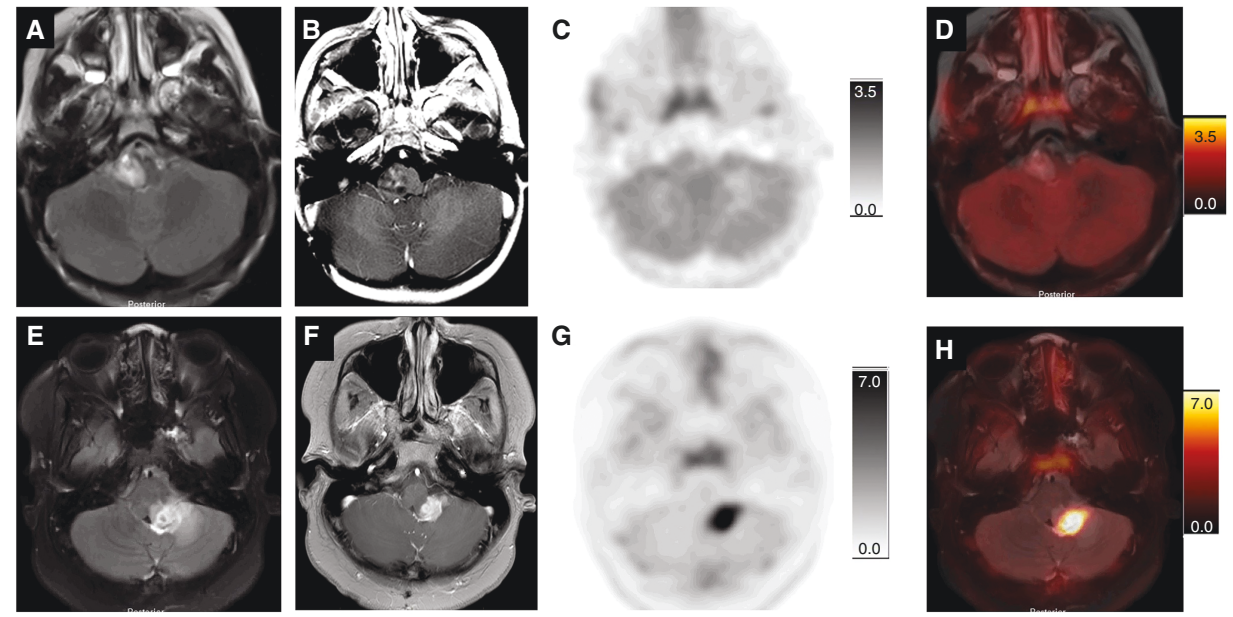

Figure 3. Pilomyxoid astrocytoma. (A-D). A) Axial FLAIR image through the posterior fossa demonstrated a T2 hyperintense tumor involving the right side of the medulla that demonstrated patchy enhancement on post-contrast T1 weighted image (B). The Attenuation corrected [11C]-MET-PET image (C) demonstrated barely any uptake of the tracer over the area of abnormality, as shown on the overlay image (D) with a TBR_{max} of 1.83. Ganglioglioma. (E-H; E) Axial FLAIR image through the posterior fossa demonstrated a T2 hyperintense tumor involving the inferior aspect of the left middle cerebellar peduncle, dorsal aspect of the inferior pons (anteriorly), and cerebellum (posteriorly) with nodular enhancement on post-contrast T1 weighted image (F). The Attenuation corrected [11C]-MET-PET image (G) demonstrated intense uptake of the tracer over the area of abnormality, as shown on the overlay image (H) with a TBR_{max} of 6.84.

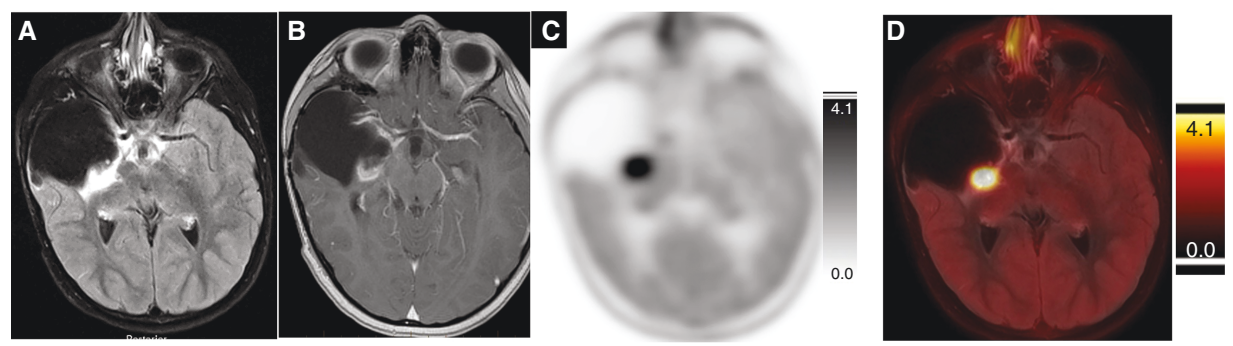

Figure 4. Fibrillary astrocytoma, previously resected. (A) Axial FLAIR image through the temporal lobe demonstrated an area of nodularity, suspicious for recurrence, at the posteromedial aspect of the large cystic resection cavity from prior resection of a large fibrillary astrocytoma, some component of which demonstrated minimal enhancement on post contrast T1 weighted image (B). The Attenuation corrected [11C]-MET-PET image (C) demonstrated intense uptake of the tracer over the focal nodularity, as shown on the overlay image (D) with a TBR_{max} of 4.27.

the BRAF-fused tumor group ($n = 5$). However, due to the small sample size, we did not perform a formal statistical test. All the tumors in both groups demonstrated contrast enhancement. In the DAs ($n = 5$), both TBR_{max} and TBR_{peak} median values were higher than those of PAs, while TBR_{mean} median value was slightly higher in PAs ($n = 7$). (Supplementary Table 6) Once again, we did not perform a formal statistical test due to the very small sample size.

Discussion

Amino acid PET imaging has become a prevalent method for assessing gliomas, particularly in adult cases. To standardize its application in both adult and pediatric brain tumors, working groups such as RANO (Response Assessment in Neuro-oncology), RAPNO, and SIOPE have collaborated with Society of Nuclear Medicine and

Table 1. Sensitivity of [11C]-MET-PET for Diagnosing pLGG

Index	Qualitative PET interpretation	TBR_{max}	TBR_{mean}	TBR_{peak}
Sensitivity (95% CI) -newly diagnosed	0.93(0.66, 1)	0.87 (0.58,0.98)	0.67 (0.39, 0.87)	0.87 (0.58,0.98)
Sensitivity (95% CI)- previously treated	0.96 (0.78, 1)	0.96 (0.78, 1)	0.81 (0.6, 0.93)	0.96 (0.78, 1)
Sensitivity (95% CI)- combined	0.95 (0.82, 0.99)	0.93 (0.79, 0.98)	0.76 (0.59, 0.87)	0.93 (0.79, 0.98)

Table 2. [11C]-MET-PET Done Both Before and After Therapy in Patients Who Had MET-PET Done Both Before and After Therapy (Newly Diagnosed [*n* = 9] and in Previously Treated Group [*n* = 7])

	Newly diagnosed pretherapy median (range)	Newly diagnosed post-therapy median (range)	Previously treated pretherapy median (range)	Previously treated post-therapy median (range)	Combined pretherapy Median (range)	Combined post-therapy median (range)
TBR_{max}	2 (1.46–4.17)	2 (1.46–3.92)	2.7 (1.57–4)	2.46 (1.64–4.2)	2.6 (1.46–4.17)	2.24* (1.46–4.2)
TBR_{peak}	1.78 (1.31–3.92)	1.6 (1.36–3.67)	2.1 (1.43–3.7)	2.15 (1.36–3.9)	2.05 (1.31–3.92)	1.83 (1.36–3.9)
TBR_{mean}	1.42 (0.85–2.17)	1.46 (0.86–2.11)	1.7 (1–2.2)	1.67 (0.91–2.1)	1.6 (0.85–2.2)	1.5 (0.86–2.11)
MTV (in mL)	6 (0.13–73.5)	4.7 (0.34–44.2)	3.5 (0.41–33.3)	2.1 (0.14–35.1)	5.8 (0.13–73.5)	3.4 (0.14–44.2)
FLAIR volume (in mL)	11.4 (5.8–81)	11* (0.49–49)	7.5 (2.5–58.9)	3.6 (1.2–42.6)	10.2 (2.5–81)	8.85* (0.49–49)

*P < .05, TBR, tumor-to-brain ratio; MTV, metabolic tumor volume.

Molecular Imaging and EANM to establish practice guidelines for this imaging technique.[28,40] [11C]-MET, [18F]-FET, and [18F]-DOPA are the most widely used amino acid PET tracers in brain tumor imaging. While these radiotracers share similar transport mechanisms, entering tumor tissue through L-amino acid transporters, they exhibit different metabolic fates within tumors, leading to distinct applications in tumor imaging.[41] No specific guideline recommends one amino acid PET tracer over another, as [11C]-MET and [18F]-FET can offer comparable diagnostic information.[42,43] If a choice is available, [11C]-MET presents rapid uptake with minimal background activity or metabolism, enabling the acquisition of high-quality images soon after injection. However, more [11C]-MET-PET data are required to use this technique routinely for pLGGs. This study aims to contribute additional data in this regard.

In this study, we found that qualitative and quantitative [11C]-MET-PET exhibits high sensitivity in diagnosing pLGGs (pediatric low-grade gliomas). Moreover, we observed a trend of therapy-associated decrease in quantitative [11C]-MET-PET parameters. However, this trend did not reach statistical significance due to the small sample size. Additionally, in another small subgroup descriptive analysis, we identified that *BRAF pV600E*-mutant tumors tend to show slightly higher [11C]-MET-PET uptake than *BRAF*-fused tumors. These results indicate that a positive [11C]-MET-PET study, either quantitative or qualitative, suggests the presence of tumor and can be used to complement an inconclusive MRI. Similar findings of [11C]-MET-PET were reported in pHGG[13] and DIPG[36] and in adult-type low-grade glioma.[44] Although the median TBR_{max} and TBR_{mean} of the newly diagnosed pLGGs in our study are similar to those of previously treated pLGGs, and the respective values are different from the adult low-grade gliomas.[45] Median TBR_{max} of the combined cohort in our study, though, is higher than the threshold values (TBR = 2.11) used previously to differentiate grades 2 and 3 gliomas in adults.[46]

In both the non-newly diagnosed and previously treated groups, analyzed independently, there were no statistically significant differences between the pre- and post-therapy quantitative [11C]-MET-PET parameters. This indicates that the data distributions remained consistent before and after the initial treatment. However, it is essential to note that the limited number of patients in the study may have influenced the results, and further investigations with larger sample sizes are warranted for more robust conclusions.

However, when we combined data from both the newly diagnosed and previously treated groups, the change in TBR_{max} median value from pre- to post-therapy reached statistical significance ($P = .03$). This observation suggests that the TBR_{max} values before and after therapy do not have identical distributions and may be linked to therapeutic intervention.

In our study, we observed that pLGGs with BRAF V600E alteration and diffuse astrocytomas tended to show higher quantitative PET parameters when compared to BRAF-fused pLGGs and PAs, respectively. Apart from a case report describing a mismatch between FDG and [11C]-MET uptake in polymorphous low-grade neuroepithelial tumor of the young,[47] and low [11C]-MET uptake in dysembryoplastic neuroepithelial tumors,[48,49] no other study has yet reported patterns of [11C]-MET uptake in pLGGs.

Using a standardized quantitative PET image analysis, our study has demonstrated that the median TBR_{max} and TBR_{mean} values in different types of newly diagnosed pLGGs differ from those reported in adult *IDH*-mutated low-grade gliomas.[45,46] These findings suggest that the [11C]-MET uptake patterns in pLGGs may not mirror those observed in adult low-grade gliomas. As a result, relying on [11C]-MET-PET values obtained from adult low-grade gliomas to assess pLGGs may not be ideal. Considering these differences, we recommend a cautious approach when using the available quantitative PET parametric references based on adult low-grade gliomas. This is crucial, as pLGGs are biologically different from adult low-grade gliomas.[50] Accurate evaluation and treatment decisions require a comprehensive understanding and awareness of these distinctions.

Our study has several limitations. Study enrollment bias exists, as the inclusion criteria for obtaining [11C]-MET-PET was based on a high suspicion of active brain tumor, either clinically, radiographically, or both. Therefore, the pretest probability was high in our study sample. A larger, prospective multi-institutional study of pediatric patients with [11C]-MET-PET may reduce this selection bias. The small sample size is another limitation.

In summary, our study reveals the high sensitivity of [11C]-MET-PET in diagnosing both newly diagnosed and recurrent pLGGs. Additionally, our findings suggest that chemotherapy and radiation therapy can reduce [11C]-MET uptake in pLGGs. Moreover, we observed potential variations in [11C]-MET uptake patterns among different histologic phenotypes and genotypes of pLGGs. However, a study with a larger cohort is desirable to establish and validate these findings.

Supplementary material

Supplementary material is available online at *Neuro-Oncology* (https://academic.oup.com/neuro-oncology).

Keywords

[11C]-MET PET | amino acid PET | pediatric-type low-grade glioma

Funding

EK's work on the project was through Pediatric Oncologic Education (POE) training funded by National Institutes of Health (#R25CA023944). JC receives support from the St. Jude Comprehensive Cancer Center (NCI grant P30CA021765), NCI Program Project P01CA096832. AKB received support from FDA grant (FD006368-01A1). This project was also supported, in part, by American Lebanese Syrian Associated Charities (ALSAC). The content is solely the responsibility of the authors and does not necessarily represent the official views of the National Institutes of Health.

Acknowledgment

We would like to thank the Molecular Imaging Core staff for the routine production of [11C]methionine. We thank Cherise Guess, PhD, ELS, for scientific editing.

Conflict of interest statement

Financial disclosure: No potential conflicts of interest relevant to this article exist. *Disclaimer:* The content is solely the responsibility of the authors and does not necessarily represent the official views of the National Institutes of Health.

Authorship statement

Study design: A.B.; Study Conduct: E.K., A.B., and B.S.; patient recruitment: I.Q., T.M., G.W., andB.S.; tracer production: A.V. and S.S.; Image analysis: E.K., J.H., A.B., and B.S.; pathology and molecular diagnosis: J.C.; statistical analysis: Y.L. and T.P.; manuscript writing: E.K. and A.B.; manuscript reviewing: E.K., A.B., B.S., A.V., S.S., T.M., G.W., A.V., S.S. Y.L., T.P., and J.C.. *Disclaimer:* None. *Financial Support:* EK worked on the project as a Pediatric Oncologic Education (POE) training funded by National Institute of Health (#R25CA023944). JC receives support from the St. Jude Comprehensive Cancer Center (NCI grant P30CA021765), NCI Program Project P01CA096832. AKB received support from FDA grant (FD006368-01A1). This project was also partially supported by American Lebanese Syrian Associated Charities. The content is solely the responsibility of the authors and does not necessarily represent the official views of the National Institutes of Health.

Affiliations

Department of Diagnostic Imaging, St. Jude Children's Research Hospital, Memphis, Tennessee, USA (E.Y.K., A.L.V., S.E.S.J.H., B.L.S., A.K.B.); Department of Pathology, St. Jude Children's Research Hospital, Memphis, Tennessee, USA (J.C.); Department of Biostatistics, St. Jude Children's Research Hospital, Memphis, Tennessee, USA (Y.L., T.P.); Department of Oncology, St. Jude Children's Research Hospital, Memphis, Tennessee, USA (I.Q., G.W.R.); Department of Radiation Oncology, St. Jude Children's Research Hospital, Memphis, Tennessee, USA (T.E.M.)

References

1. Diwanji TP, Engelman A, Snider JW, Mohindra P. Epidemiology, diagnosis, and optimal management of glioma in adolescents and young adults. *Adolesc Health Med Ther.* 2017;8(Sep 22):99–113.

2. Fangusaro J, Witt O, Hernaiz Driever P, et al. Response assessment in paediatric low-grade glioma: Recommendations from the Response Assessment in Pediatric Neuro-Oncology (RAPNO) working group. *Lancet Oncol.* 2020;21(6):e305–e316.
3. Kim HJ, McLawhorn AS, Goldstein MJ, Boland PJ. Malignant osseous tumors of the pediatric spine. *J Am Acad Orthop Surg.* 2012;20(10):646–656.
4. Louis DN, Perry A, Wesseling P, et al. The 2021 WHO classification of tumors of the central nervous system: A summary. *Neuro Oncol.* 2021;23(8):1231–1251.
5. de Blank P, Bandopadhayay P, Haas-Kogan D, Fouladi M, Fangusaro J. Management of pediatric low-grade glioma. *Curr Opin Pediatr.* 2019;31(1):21–27.
6. Ryall S, Zapotocky M, Fukuoka K, et al. Integrated molecular and clinical analysis of 1,000 pediatric low-grade gliomas. *Cancer Cell.* 2020;37(4):569–583.e5.
7. Li X, Moreira DC, Bag AK, et al. The clinical and molecular characteristics of progressive hypothalamic/optic pathway pilocytic astrocytoma. *Neuro Oncol.* 2023;25(4):750–760.
8. Wisoff JH, Sanford RA, Heier LA, et al. Primary neurosurgery for pediatric low-grade gliomas: A prospective multi-institutional study from the Children's Oncology Group. *Neurosurgery.* 2011;68(6):1548–54; discussion 1554. discussion 15545.
9. Shaw EG, Wisoff JH. Prospective clinical trials of intracranial low-grade glioma in adults and children. *Neuro Oncol.* 2003;5(3):153–160.
10. Krishnatry R, Zhukova N, Guerreiro Stucklin AS, et al. Clinical and treatment factors determining long-term outcomes for adult survivors of childhood low-grade glioma: A population-based study. *Cancer.* 2016;122(8):1261–1269.
11. Naftel RP, Pollack IF, Zuccoli G, Deutsch M, Jakacki RI. Pseudoprogression of low-grade gliomas after radiotherapy. *Pediatr Blood Cancer.* 2015;62(1):35–39.
12. Deuschl C, Kirchner J, Poeppel TD, et al. (11)C-MET PET/MRI for detection of recurrent glioma. *Eur J Nucl Med Mol Imaging.* 2018;45(4):593–601.
13. Bag AK, Wing MN, Sabin ND, et al. (11)C-Methionine PET for identification of pediatric high-grade glioma recurrence. *J Nucl Med.* 2022;63(5):664–671.
14. Reardon DA, Weller M. Pseudoprogression: Fact or wishful thinking in neuro-oncology? *Lancet Oncol.* 2018;19(12):1561–1563.
15. Slavc I, Chocholous M, Leiss U, et al. Atypical teratoid rhabdoid tumor: improved long-term survival with an intensive multimodal therapy and delayed radiotherapy. The Medical University of Vienna Experience 1992-2012. *Cancer Med.* 2014;3(1):91–100.
16. la Fougere C, Suchorska B, Bartenstein P, Kreth FW, Tonn JC. Molecular imaging of gliomas with PET: Opportunities and limitations. *Neuro Oncol.* 2011;13(8):806–819.
17. Katsanos AH, Alexiou GA, Fotopoulos AD, et al. Performance of 18F-FDG, 11C-Methionine, and 18F-FET PET for glioma grading: A Meta-analysis. *Clin Nucl Med.* 2019;44(11):864–869.
18. Albert NL, Weller M, Suchorska B, et al. Response assessment in neuro-oncology working group and European Association for Neuro-Oncology recommendations for the clinical use of PET imaging in gliomas. *Neuro Oncol.* 2016;18(9):1199–1208.
19. Preuss M, Werner P, Barthel H, et al. Integrated PET/MRI for planning navigated biopsies in pediatric brain tumors. *Childs Nerv Syst.* 2014;30(8):1399–1403.
20. Hotta M, Minamimoto R, Miwa K. 11C-methionine-PET for differentiating recurrent brain tumor from radiation necrosis: Radiomics approach with random forest classifier. *Sci Rep.* 2019;9(1):15666.
21. Galldiks N, Kracht LW, Burghaus L, et al. Use of 11C-methionine PET to monitor the effects of temozolomide chemotherapy in malignant gliomas. *Eur J Nucl Med Mol Imaging.* 2006;33(5):516–524.
22. Galldiks N, Niyazi M, Grosu AL, et al. Contribution of PET imaging to radiotherapy planning and monitoring in glioma patients - A report of the PET/RANO group. *Neuro Oncol.* 2021;23(6):881–893.
23. Morana G, Piccardo A, Puntoni M, et al. Diagnostic and prognostic value of 18F-DOPA PET and 1H-MR spectroscopy in pediatric supratentorial infiltrative gliomas: A comparative study. *Neuro Oncol.* 2015;17(12):1637–1647.
24. Marner L, Lundemann M, Sehested A, et al. Diagnostic accuracy and clinical impact of [18F]FET PET in childhood CNS tumors. *Neuro Oncol.* 2021;23(12):2107–2116.
25. Misch M, Guggemos A, Driever PH, et al. (18)F-FET-PET guided surgical biopsy and resection in children and adolescence with brain tumors. *Childs Nerv Syst.* 2015;31(2):261–267.
26. Kertels O, Krauss J, Monoranu CM, et al. [(18)F]FET-PET in children and adolescents with central nervous system tumors: Does it support difficult clinical decision-making? *Eur J Nucl Med Mol Imaging.* 2023;50(6):1699–1708.
27. Dunkl V, Cleff C, Stoffels G, et al. The usefulness of dynamic O-(2-18F-fluoroethyl)-L-tyrosine PET in the clinical evaluation of brain tumors in children and adolescents. *J Nucl Med.* 2015;56(1):88–92.
28. Piccardo A, Albert NL, Borgwardt L, et al. Joint EANM/SIOPE/RAPNO practice guidelines/SNMMI procedure standards for imaging of paediatric gliomas using PET with radiolabelled amino acids and [(18)F]FDG: Version 1.0. *Eur J Nucl Med Mol Imaging.* 2022;49(11):3852–3869.
29. Pirotte B, Goldman S, Dewitte O, et al. Integrated positron emission tomography and magnetic resonance imaging-guided resection of brain tumors: A report of 103 consecutive procedures. *J Neurosurg.* 2006;104(2):238–253.
30. Chung JK, Kim YK, Kim SK, et al. Usefulness of 11C-methionine PET in the evaluation of brain lesions that are hypo- or isometabolic on 18F-FDG PET. *Eur J Nucl Med Mol Imaging.* 2002;29(2):176–182.
31. Kato T, Shinoda J, Oka N, et al. Analysis of 11C-methionine uptake in low-grade gliomas and correlation with proliferative activity. *AJNR Am J Neuroradiol.* 2008;29(10):1867–1871.
32. Kracht LW, Friese M, Herholz K, et al. Methyl-[11C]- l-methionine uptake as measured by positron emission tomography correlates to microvessel density in patients with glioma. *Eur J Nucl Med Mol Imaging.* 2003;30(6):868–873.
33. Smits A, Westerberg E, Ribom D. Adding 11C-methionine PET to the EORTC prognostic factors in grade 2 gliomas. *Eur J Nucl Med Mol Imaging.* 2008;35(1):65–71.
34. Herholz K, Holzer T, Bauer B, et al. 11C-methionine PET for differential diagnosis of low-grade gliomas. *Neurology.* 1998;50(5):1316–1322.
35. Yamane T, Sakamoto S, Senda M. Clinical impact of (11)C-methionine PET on expected management of patients with brain neoplasm. *Eur J Nucl Med Mol Imaging.* 2010;37(4):685–690.
36. Tinkle CL, Duncan EC, Doubrovin M, et al. Evaluation of (11)C-methionine PET and anatomic MRI associations in diffuse intrinsic pontine glioma. *J Nucl Med.* 2019;60(3):312–319.
37. Singhal T, Narayanan TK, Jacobs MP, Bal C, Mantil JC. 11C-methionine PET for grading and prognostication in gliomas: A comparison study with 18F-FDG PET and contrast enhancement on MRI. *J Nucl Med.* 2012;53(11):1709–1715.
38. Vāvere AL, Snyder SE. Synthesis of L-[methyl-11C]methionine ([11C] MET). **In:** Scott PJH, Hockley BG, eds. Radiochemical Syntheses : Radiopharmaceuticals for Positron Emission Tomography. John Wiley & Sons, Inc; 2012:199–212. doi: 10.1002/9781118140345.ch20
39. Li Z, Chen YA, Chow D, et al. Practical applications of CISS MRI in spine imaging. *Eur J Radiol Open.* 2019;6(June 27):231–242.
40. Law I, Albert NL, Arbizu J, et al. Joint EANM/EANO/RANO practice guidelines/SNMMI procedure standards for imaging of gliomas using PET with radiolabelled amino acids and [(18)F]FDG: Version 1.0. *Eur J Nucl Med Mol Imaging.* 2019;46(3):540–557.
41. Juhasz C, Dwivedi S, Kamson DO, Michelhaugh SK, Mittal S. Comparison of amino acid positron emission tomographic radiotracers for molecular

imaging of primary and metastatic brain tumors. *Mol Imaging.* 2014;13:10.2310/7290.2014.00015.

42. Weber WA, Wester HJ, Grosu AL, et al. O-(2-[18F]fluoroethyl)-L-tyrosine and L-[methyl-11C]methionine uptake in brain tumours: Initial results of a comparative study. *Eur J Nucl Med.* 2000;27(5):542–549.
43. Grosu AL, Astner ST, Riedel E, et al. An interindividual comparison of O-(2-[18F]fluoroethyl)-L-tyrosine (FET)- and L-[methyl-11C]methionine (MET)-PET in patients with brain gliomas and metastases. *Int J Radiat Oncol Biol Phys.* 2011;81(4):1049–1058.
44. Braun V, Dempf S, Weller R, et al. Cranial neuronavigation with direct integration of (11)C methionine positron emission tomography (PET) data -- results of a pilot study in 32 surgical cases. *Acta Neurochir (Wien).* 2002;144(8):777–82; discussion 782. discussion 782.
45. Ninatti G, Sollini M, Bono B, et al. Preoperative [11C]methionine PET to personalize treatment decisions in patients with lower-grade gliomas. *Neuro Oncol.* 2022;24(9):1546–1556.
46. Poetsch N, Woehrer A, Gesperger J, et al. Visual and semiquantitative 11C-methionine PET: An independent prognostic factor for survival of newly diagnosed and treatment-naive gliomas. *Neuro Oncol.* 2018;20(3):411–419.
47. Tateishi K, Ikegaya N, Udaka N, et al. BRAF V600E mutation mediates FDG-methionine uptake mismatch in polymorphous low-grade neuroepithelial tumor of the young. *Acta Neuropathol Commun.* 2020;8(1):139.
48. Rosenberg DS, Demarquay G, Jouvet A, et al. [11C]-Methionine PET: Dysembryoplastic neuroepithelial tumours compared with other epileptogenic brain neoplasms. *J Neurol Neurosurg Psychiatry.* 2005;76(12):1686–1692.
49. Kaplan AM, Lawson MA, Spataro J, et al. Positron emission tomography using [18F] fluorodeoxyglucose and [11C] l-methionine to metabolically characterize dysembryoplastic neuroepithelial tumors. *J Child Neurol.* 1999;14(10):673–677.
50. Greuter L, Guzman R, Soleman J. Pediatric and adult low-grade gliomas: Where do the differences lie? *Children (Basel).* 2021;8(11):1075.